Speed of Line Protection – Can We Break Free of Phasor Limitations?

Edmund O. Schweitzer, III, Bogdan Kasztenny, Armando Guzmán,
Veselin Skendzic, and Mangapathirao V. Mynam
Schweitzer Engineering Laboratories, Inc.

This paper was presented at the 68th Annual Conference for Protective Relay Engineers and can be accessed at: http://dx.doi.org/10.1109/CPRE.2015.7102184.

For the complete history of this paper, refer to the next page.

Published in
Locating Faults and Protecting Lines at the Speed of Light: Time-Domain Principles Applied, 2018

Previously presented at the
69th Annual Georgia Tech Protective Relaying Conference, April 2015,
and 68th Annual Conference for Protective Relay Engineers, March 2015

Originally presented at the
41st Annual Western Protective Relay Conference, October 2014

Speed of Line Protection – Can We Break Free of Phasor Limitations?

Edmund O. Schweitzer, III, Bogdan Kasztenny, Armando Guzmán, Veselin Skendzic, and Mangapathirao V. Mynam, *Schweitzer Engineering Laboratories, Inc.*

***Abstract*—Today's relays are predominantly based on phasors, and as such, they incur a delay associated with the full-cycle observation window required for accurate phasor estimation. Considerable improvement in speed is possible by using information in the transients of voltages and currents. We review a number of protection techniques, including directional elements, direct tripping underreaching elements, and differential elements that significantly speed up line protection.**

I. Introduction

Power system stability has driven the quest for faster transmission line protection. Faults must be cleared faster than the critical fault clearing time or else the system may lose transient stability and possibly black out. Faster fault clearing increases the amount of power that can be transferred.

Primary protective relaying systems typically operate in one to one-and-a-half cycles, and the breakers interrupt current in one-and-a-half to three cycles, so faults are typically cleared in three to four cycles. Sometimes the relaying system operates faster. For example, sensitive instantaneous overcurrent elements can be used for switch-onto-fault events, and we have observed them operate in one-quarter of a cycle. However, when we consider stability limits for planning purposes, we must assume conservative protection operating times.

If a breaker fails to trip, breaker failure schemes take over, and fault clearing is delayed until the slowest backup breaker operates, which may be around 10 to 12 cycles. If time-coordinated remote backup protection is used instead of breaker failure protection, the fault clearing time may be as high as a few hundred milliseconds.

Every millisecond saved in fault clearing time means more power can be transferred. A 1976 BPA paper shows that on a particular line, a one-cycle reduction in fault clearing time increased the power transfer by 250 MW, amounting to about 15 MW per millisecond [1]. Put another way, every millisecond saved may be on the order of another distribution feeder served!

Faster protection also enhances public and utility personnel safety, limits equipment wear, improves power quality, and reduces property damage.

Most protection principles are based on the fundamental frequency components of voltages and currents. Accurate measurement of a sinusoidal quantity typically takes a cycle. So, to consistently trip faster, we must also consider transient components. And, we should also revisit how and what we communicate end to end for communications-based line protection.

Fast relays, by their nature, respond to high-frequency signal components, which brings additional benefits. Consider nontraditional sources (such as wind and solar). These sources have no inertia and are connected to the power system through a power electronics interface. Their control algorithms protect the converters for network fault conditions. As a result, these sources produce voltages and currents that challenge some protection principles developed for networks with synchronous generators. Relays responding to transients are inherently less dependent on the sources and more dependent on the network itself. Thus they promise to be useful in applications near nontraditional sources.

Because series capacitors initially appear to be short circuits during faults, relays designed to operate on the transient component of the fault generally perform better in series-compensated line applications.

Faults launch traveling waves (TWs) that travel close to the speed of light and get reflected and transmitted at buses and other discontinuities according to their corresponding characteristic impedances. In the initial stage of the fault, the power system behaves as a distributed parameter network. The TWs are well described by the propagation velocity, the reflection and transmission coefficients, and the line characteristic impedance. TWs can be used to provide ultra-high-speed protection, with possible operating times that are below 1 millisecond. The speed of light is the limiting factor. TWs from a fault anywhere on a 100-mile line reach both ends within 600 microseconds.

After a few roundtrip reflections, TWs recombine into stationary waves, and the power system starts to look like a lumped parameter RLC network in a transient state. The protection system can analyze the "lumped circuit theory" transient waveforms and reliably operate in milliseconds.

Incremental quantities—signals that appear due to a fault and do not contain load voltages or currents—simplify the line and system representation by eliminating power sources and leaving the fault as the only "source" in the equivalent network. Put another way, the driving force of the transient is the fault, and the driving force of the steady-state response is the set of system fundamental frequency sources (e.g., generators).

The traditional frequency domain techniques obtained by extracting fundamental frequency components (phasors) apply

later when the signals settle down. The filtering necessary for phasor measurement results in operating times of about one power cycle, with the best-case times approaching half a cycle for close-in high-current faults.

Ultra-high-speed principles allow relays to see events that are located within the protected zone but are not necessarily permanent faults. Incipient cable failures or surge arrester conduction events can challenge today's feeder and bus relays, respectively. Similarly, the ultra-high-speed line protection needs to ensure that an in-zone event is a legitimate fault.

II. Speed of Conventional Protection Elements

Most power system faults are cleared by routine protection system operation. The two major fault clearing time components are:

- Fault detection time, defined as the time from the fault inception to the moment when a relay contact closes to initiate breaker tripping. This is the protection scheme operating time, which includes the delays caused by the protective relays, communications channels, and auxiliary relays (when used).
- Fault current interruption time, defined as the time from the moment when the breaker coil is energized to the moment when the primary current is completely interrupted. This is the breaker interrupting time, which is the sum of the breaker opening and arcing times.

Today's breakers provide for two-cycle interrupting times. Modern digital channels have a latency of around 1 millisecond for direct fiber and a quarter- to half-a-cycle for analog and network-based channels. Relay operating times vary with the system and fault conditions, but they are typically between one cycle and one-and-a-half cycles.

A. Phasor-Based Protection Element Implementations

Most electromechanical, solid-state, and microprocessor-based relays effectively operate on phasor-based principles.

Relays using phasors apply filtering so that they respond to the fundamental frequency signal components. Their operating principles are derived assuming the filtered signals have near-sinusoidal waveforms.

Let us look at the microprocessor-based mho element. This element performs the phase comparison of an operating signal, given by (1), and a chosen polarizing signal to obtain the operating characteristic shown in Fig. 1. The memorized positive-sequence voltage $V_{1(mem)}$ is often used for polarization, as in (2). In these equations, the voltage and current signals are phasors.

$$V_{OP} = m_0 \bullet Z_R \bullet I - V \quad (1)$$

$$V_{POL} = V_{1(mem)} \quad (2)$$

where:

Z_R is the line replica impedance.

m_0 is the per-unit (pu) reach in terms of Z_R.

I is the measured loop current.

V is the measured loop voltage.

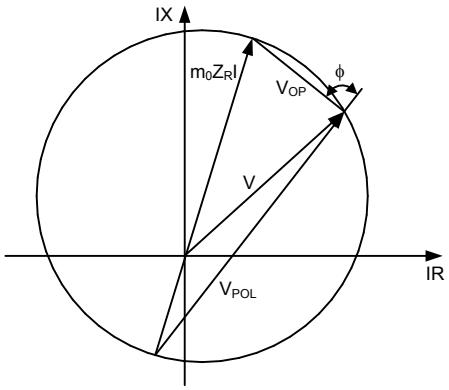

Fig. 1. Mho element characteristic.

Mathematically, the mho operating characteristic is the locus (a circle) for which the angle between the operating and polarizing quantities ϕ equals ±90 degrees. The element operating region (the area inside the circle in Fig. 1) is defined for angle values between –90 degrees and +90 degrees.

Fig. 2 is a simplified functional block diagram of the mho element in a microprocessor-based relay. The analog low-pass filters reject the signal higher-frequency components. The digital band-pass filters obtain the fundamental frequency component of the signals and reject harmonics and the exponentially decaying dc offset component [2].

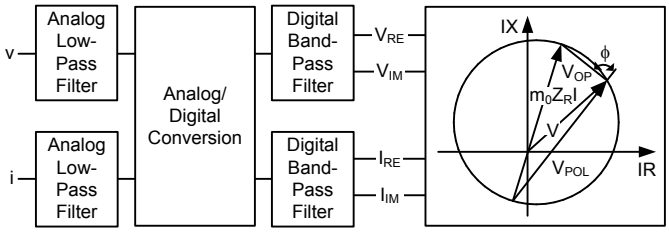

Fig. 2. Microprocessor-based mho element.

In a microprocessor-based mho element, the phasors are measured explicitly and the mho element theory can be used directly for implementation, such as following (1) and (2). Actual implementations optimize the numerical operations, such as calculating a torque-like product $\mathrm{Re}\left(V_{OP} \bullet V_{POL}^{*}\right)$ instead of checking the angle between (1) and (2) [3]. Yet another alternative is to calculate the distance to the fault value (m) and compare it with the reach setting (m_0) [4] [5]. In any case, the implementation includes the phasor estimation process that requires band-pass filtering.

The need for filtering is not unique to microprocessor-based relays. Filtering allowing the application of near-sinusoidal signal assumptions to create protection elements has been accomplished by:

- Operating torque averaging of the moving relay armature in the electromechanical relay technology.
- Explicit analog band-pass filtering in the solid-state relay technology.
- Explicit digital band-pass filtering in the microprocessor-based relay technology.

Limiting the transient overshoot for the signals of interest (the fundamental frequency band) implies a filter latency on the order of one power cycle. We can understand this simply from the following observation: in order to accurately measure a frequency component, we need to observe this component for the duration of its cycle. One of the authors likes to say that "it takes a cycle to catch a cycle."

B. Half-Cycle and Variable Data Window Algorithms

Some practical microprocessor-based relays today use a half-cycle data window for phasor estimation. Half-cycle phasor estimators are faster than full-cycle estimators but have higher transient errors (overshoot) because accuracy is traded for speed when shortening the filter window. These implementations recognize the higher transient estimation errors and accommodate them by applying larger margins to the protection element settings. For example, the half-cycle phasor estimators of a distance element can provide high-speed coverage of around 80 percent of the Zone 1 reach setting (e.g., 64 percent of the line length for an 80 percent reach setting).

These half-cycle distance elements operate quickly, especially for close-in faults. For example, a solution described in [6] achieves typical operating times of 8 milliseconds for close-in faults on a 60 Hz system, 11 milliseconds for faults at 70 percent of the line length, and 24 milliseconds for faults at the end of the line.

A similar approach is to use variable data windows: resize the phasor estimator to a short window upon fault detection for speed, and after some time, increase the size of the window to a full design length [7]. When the window is shorter than the full design length, the relay applies extra security margins.

We conclude that the use of power system frequency components for protection provides operating times in the order of half a cycle for close-in faults, about one cycle for typical fault conditions, and about one-and-a-half cycles for faults near the end of the protection zone. Good relay design traditionally trades off speed for accuracy for faults near the end of the zone.

C. Protection Elements With Low Accuracy Requirements

There are applications where accuracy is less important, such as the following:

- Switch-onto-fault logic, where the line can be tripped securely using overcurrent elements that are set relatively low compared with the fault current.
- Overreaching distance elements.
- Differential elements, especially for short lines with negligible charging current and when current transformer (CT) saturation is addressed by relay design.

In these applications, we can use half-cycle phasor estimators to gain speed. Unfortunately, these applications are not very common (switch onto a fault) or require communications for tripping (directional comparison or current differential) and are slowed down by channel latency.

In all other applications, we need certain phasor accuracy for correct protection operation, and therefore, we have no choice but to accept delays associated with accurate phasor estimation.

D. Impact of Instrument Transformers and Signal Impairments

Instrument transformers add their own distortion to the relay input signals.

CT saturation may affect the security and dependability of overcurrent elements, distance elements, or line current differential elements. Similarly, coupling capacitor voltage transformer (CCVT) transients challenge the security of underreaching distance elements. Therefore, extra filtering or a short time delay are often part of the relay design, preventing fast relay operation.

III. Time-Domain Line Protection

In this section, we present the operation principles of several ultra-high-speed time-domain protection elements: a direct tripping underreaching element, a supervisory overreaching element, and two types of directional elements.

A. Incremental Quantities

In his 1883 paper, Léon Charles Thévenin taught that any linear stationary dc network can be represented—for any two terminals in the network—by an equivalent source and an equivalent resistance. Later on, capitalizing on Steinmetz's work on ac networks, Thévenin's theorem was extended to ac networks represented by lumped parameters and driven by stationary ac sources.

Assuming a fault between two terminals in the network, we can use Thévenin's theorem—together with the principle of superposition—to solve the faulted network. We solve it by analyzing separately the prefault network to obtain the prefault (load) components of the voltages and currents and the fault network to obtain the fault-generated components of these voltages and currents. The final solution—voltages and currents at any point in the faulted network—is the sum of the prefault and fault-generated components.

The prefault network is in the steady state. The fault network has only one source—the Thévenin source at the fault location. The Thévenin source voltage equals the negative of the voltage at the fault point in the prefault network.

Fig. 3 illustrates this approach. The fault network contains fault voltages and currents (incremental quantities). Before the fault, this equivalent network is not energized and all of its voltages and currents are zero. When the fault occurs, this network goes through a transient state and eventually settles into the fault steady state. We can solve the fault network for the steady-state values or for the transient values. The incremental quantities are valid for both states.

The superposition theorem is more than just a convenient method to solve electric circuits. It also facilitates protection techniques based on the fault-generated components of the voltages and currents. Fault-generated signal components are not affected by load but are driven by the Thévenin source in

the fault network located at the fault point. These quantities depend only on the network parameters. The only effect of the power system sources and load flow is establishing the initial conditions for the superposition (Thévenin) source.

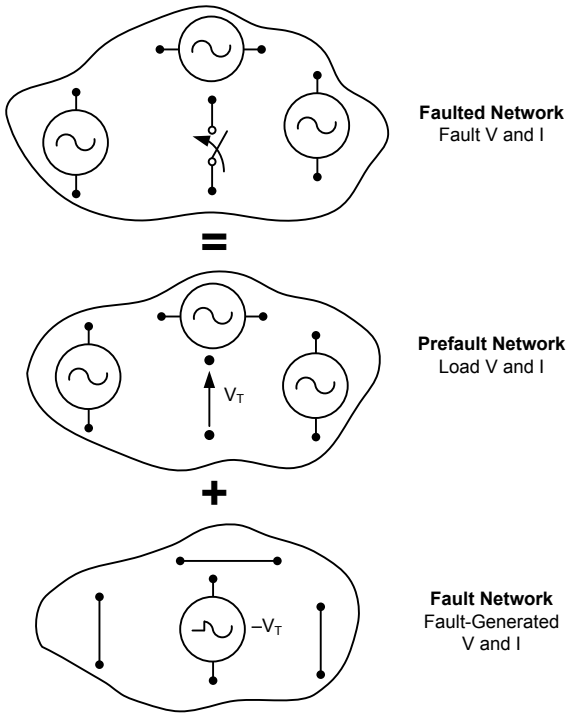

Fig. 3. Illustration of the application of the superposition and Thévenin's theorems for fault analysis.

Because the fault signals are sums of the prefault signals and the fault-generated signals (see Fig. 3), the fault-generated signals are the difference between the fault signals and the prefault signals. Relays measure the fault signals directly—these are the instantaneous voltages and currents at the relay terminals. Relays also measure the prefault signals and can extrapolate them forward in time. This extrapolation is valid only for a few tens of milliseconds because the power system sources only remain stationary for a short period of time. Therefore, one simple method to derive incremental quantities is:

$$\Delta s_{(t)} = s_{(t)} - s_{(t-pT)} \tag{3}$$

where:

Δs is the instantaneous incremental quantity.

s is the measured instantaneous value.

T is the period of the measured quantity.

p is an arbitrary number of periods.

Using (3), we obtain an incremental quantity that lasts for *p* power cycles, after which this quantity expires because the historical values we subtract slide into the fault period. We select the value of *p* depending on the intended usage of the incremental quantity. For example, if we intend to use incremental quantities during two power cycles, we can select $p > 2$, such as $p = 3$.

The time-domain incremental quantities obtained from (3) contain the transients produced by the fault. These quantities do not include the prefault load. Depending on the usage of the incremental quantities, we can further filter the signal (3) to obtain the signal components of interest.

In analog relays, time-domain incremental quantities have been derived via high-pass or notch filtering. This filtering is easier to build in analog relays than the time delay required by (3). In microprocessor-based relays, it is possible to implement (3) directly. Equation (3) is more comprehensive than the analog method because it preserves all the frequency components in the incremental quantities and does not affect the output with the transient response of a high-pass or notch filter.

B. Basic Time-Domain Voltage and Current Relationships

In the time domain, consider the single-phase RL network of Fig. 4 with a fault on the line between Terminal S and Terminal R. The fault network of Fig. 5 contains incremental voltages and currents that we will use for explaining the time-domain protection principles.

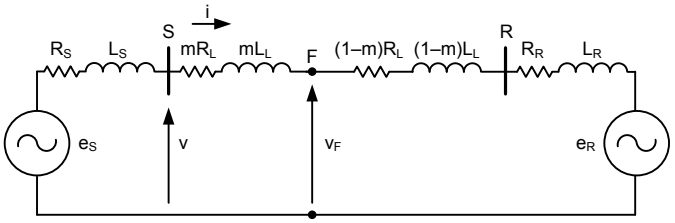

Fig. 4. Simple two-machine single-phase system with a fault at F.

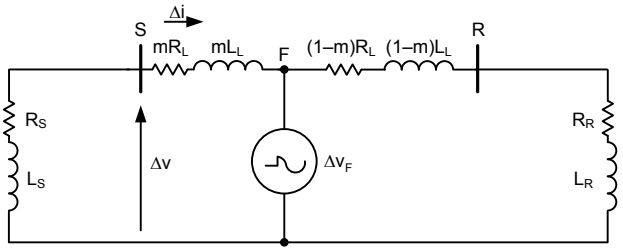

Fig. 5. Fault network of the system in Fig. 4 for analysis of incremental quantities.

At the relay location S, the incremental voltage and current are related by a voltage drop equation across the Source S resistance and inductance:

$$\Delta v = -\left(R_S \bullet \Delta i + L_S \bullet \frac{d}{dt} \Delta i \right) \tag{4}$$

Let us scale (4) for ease of further use by multiplying and dividing the right-hand side by the magnitude of the Source S impedance Z_S:

$$\Delta v = -|Z_S| \left(\frac{R_S}{|Z_S|} \bullet \Delta i + \frac{L_S}{|Z_S|} \bullet \frac{d}{dt} \Delta i \right) \tag{5}$$

We can do this operation without loss of generality because we scale function (5) with a scalar. Equation (5) includes a new current term that is a combination of the instantaneous incremental current and its derivative. Let us label this new current signal as follows:

$$\Delta i_Z = D_0 \bullet \Delta i + D_1 \bullet \frac{d}{dt}\Delta i \tag{6}$$

where:

$$D_0 = \frac{R_S}{|Z_S|} \text{ and } D_1 = \frac{L_S}{|Z_S|} \tag{7}$$

Now we can write a simple voltage-current equation for the incremental quantities measured at Terminal S:

$$\Delta v = -|Z_S| \bullet \Delta i_Z \tag{8}$$

This derivation is valid only for an RL circuit representing the line and the power system. Equation (8) has the same format as the voltage-current expression for phasors:

$$\Delta V = -Z_S \bullet \Delta I \tag{9}$$

The current given by (6) is referred to as a "replica current" and allows us to substitute for the $I \bullet Z$ terms from the frequency domain (phasors), such as (1) or (9), in the time domain (instantaneous values), such as (8). By selecting the D_0 and D_1 coefficients, as in (7), we obtain a unity gain between the measured current and the replica current at the system fundamental frequency. This unity gain is convenient for setting selection, as explained later.

We can use the network of Fig. 5 for reverse faults by placing the Δv_F source behind Terminal S. In this case, we can write the following equation between the incremental voltage and the incremental replica current:

$$\Delta v = |Z_L + Z_R| \bullet \Delta i_Z \tag{10}$$

We can explain (8), (10), and the role of the replica current by plotting the incremental voltage and the incremental replica current for forward and reverse faults, as shown in Fig. 6.

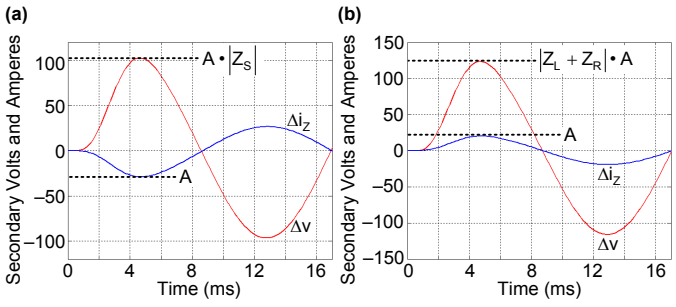

Fig. 6. Incremental voltage and incremental replica current for forward (a) and reverse (b) faults.

From Fig. 6, (8), and (10), we conclude that the incremental voltage and the incremental replica current have similar waveforms, their relative polarities indicate the fault direction, and their amplitude relationship depends on the system impedances and the fault direction. This polarity and amplitude relationship between voltage and current is similar to that of the phasor-based negative-sequence directional element (32Q; see [5]) because of our chosen scaling.

Next, we will explain how to use (8) and (10) for a time-domain ultra-high-speed directional element.

C. Directional Element

This directional protection principle was originally explored by Chamia and Liberman (see [8]) and implemented in several relays [9]. Here we will present a novel implementation using adaptive operating thresholds. We have seen that the incremental voltage and the incremental replica current have opposite polarities for forward faults and the same polarity for reverse faults. Moreover, the peak of the incremental voltage equals $|Z_S|$ times the peak of the incremental replica current for forward faults, according to (8), and it equals $|Z_L + Z_R|$ times the peak of the incremental replica current for reverse faults, according to (10). This ratio relationship holds true for any point in time, not only for peak values, if the signals are filtered well enough.

We can use this relationship to design the operating equations for the directional element.

First, let us define an instantaneous operating quantity as the product of the incremental voltage and the incremental replica current:

$$s_{OP} = \Delta v \bullet \Delta i_Z \tag{11}$$

Substituting (8) in (11), we get the expression of s_{OP} for forward faults:

$$s_{OP} = -|Z_S| \bullet (\Delta i_Z)^2 \tag{12}$$

Similarly, using (10) and (11), we obtain the expression for reverse faults:

$$s_{OP} = |Z_L + Z_R| \bullet (\Delta i_Z)^2 \tag{13}$$

The instantaneous operating signal s_{OP} is negative for forward faults and positive for reverse faults from the very first fault measurement. Theoretically, the directional element might just compare the value of s_{OP} with zero to determine the fault direction. However, we can take advantage of (12) and (13) and improve security by comparing s_{OP} with the two adaptive thresholds s_{FWD} and s_{REV}, defined by (14) and (15):

$$s_{FWD} = -Z_{FWD} \bullet (\Delta i_Z)^2 - \Delta_{MIN} \tag{14}$$

$$s_{REV} = +Z_{REV} \bullet (\Delta i_Z)^2 + \Delta_{MIN} \tag{15}$$

where Δ_{MIN} is the minimum threshold level and Z_{FWD} and Z_{REV} are relay settings. We obtain their values the same way as for the phasor-based 32Q element [5]. For example, we can use these values:

$$Z_{FWD} = 0.5 \bullet |Z_{S(MIN)}| \tag{16}$$

$$Z_{REV} = 0.5 \bullet |Z_L| \tag{17}$$

The element declares a fault to be in the forward direction when:

$$s_{OP} < s_{FWD} \tag{18}$$

The element declares a reverse direction fault when:

$$s_{OP} > s_{REV} \tag{19}$$

Equations (18) and (19) are satisfied by every sample of the fault transient period when proper filtering is applied. We may average the operating quantity s_{OP} and the adaptive thresholds s_{FWD} and s_{REV} over a short data window. This averaging does not impair or slow down operation because the involved signals develop from zero (they are based on incremental quantities) and they comply with (18) and (19) even when averaged.

Fig. 7 illustrates this directional principle for a forward fault. The operating signal is negative as expected. The forward adaptive threshold, which is selected using (16), is negative and about half the operating signal, ensuring dependable operation. The reverse adaptive threshold, which is selected using (17), is positive, ensuring a very large security margin. The operating signal and the reverse and forward adaptive thresholds are not averaged in this example. Averaging would reduce the rate of change of these signals but would not affect the relationship between the operating signal and the thresholds. The element declares a forward fault reliably per (18) in this example.

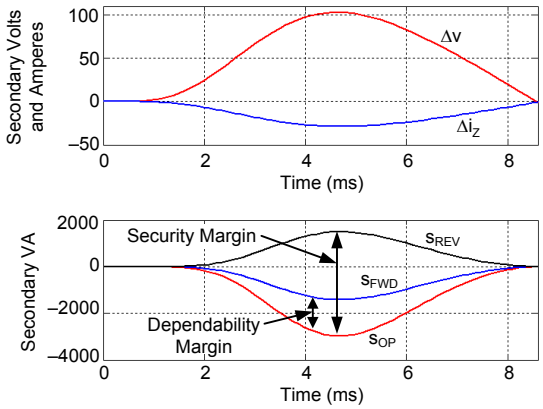

Fig. 7. Illustration of the directional element operation for a forward fault.

Proper selection of the Z_{FWD} and Z_{REV} settings allows the use of this element in applications on or near series-compensated lines [10].

D. Direct Tripping Underreaching Element

Let us now consider an element that can be set short of the remote line terminal and has proper transient overreach control so that we can use it for direct tripping without communications.

From Fig. 5, we can write the following equation for the voltage at the fault location:

$$\begin{aligned} &\Delta v - m \bullet \left|Z_L\right| \bullet \Delta i_Z = \Delta v_F \\ &\Delta v_F = v_F - v_{F(PREFAULT)} \end{aligned} \tag{20}$$

We want our element to reach up to a certain point ($m = m_0$) on the protected line short of the remote bus and not to respond to faults beyond that point. We know that the highest fault voltage change Δv_F is the system voltage V_{SYS} plus some margin. Therefore, we can selectively trip when:

$$\left|\Delta v_F\right| > k_0 \bullet V_{SYS} \tag{21}$$

where $k_0 > 1$, such as $k_0 = 1.1$.

Substituting (20) in (21), we obtain the operating equation of our underreaching element:

$$\left|\Delta v - m_0 \bullet \left|Z_L\right| \bullet \Delta i_Z\right| > k_0 \bullet V_{SYS} \tag{22}$$

The voltage at the fault point collapses very steeply during line faults. As a result, the incremental signal Δv_F exhibits a step change. The left-hand side of (22) is the measurement of $|\Delta v_F|$, and it reflects the step change of the fault point voltage. As a result, the operating equation (22) becomes satisfied quickly for in-zone faults occurring near the voltage peak, as illustrated in Fig. 8. The initial rise of the value of (22), shown in the figure, is slowed down by a digital low-pass filter that we need to use for the input voltages and currents in order to apply our protection method based on the RL line and system model. By changing the cutoff frequency of the filter, we control the balance between speed and security.

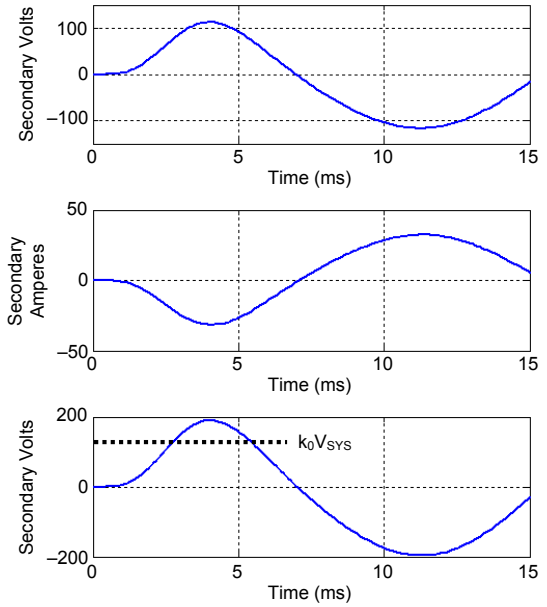

Fig. 8. Incremental voltage, incremental replica current, and operating signal for an in-zone fault occurring near the voltage peak and located at 60 percent of the set reach.

The underreaching element needs directional supervision, such as using the design described in Subsection C.

Similar elements were originally introduced by Chamia and Liberman (see [8]); Engler, Lanz, Hanggli, and Bacchini (see [11]); and Vitins (see [12]).

Here, we will further explore the response of the element based on (22) under different system conditions.

We can rearrange (8) and (22) to show the element operating characteristic on the incremental voltage versus incremental replica current plane. Let us consider the following form of (22):

$$\left|\frac{\Delta v}{m_0} - \left|Z_L\right| \bullet \Delta i_Z\right| > \frac{k_0 \bullet V_{SYS}}{m_0} \tag{23}$$

We can also express (8) in terms of the product of the line impedance and the replica current:

$$\Delta v = -\left|Z_S\right| \bullet \Delta i_Z = -\frac{\left|Z_S\right|}{\left|Z_L\right|}\left|Z_L\right| \bullet \Delta i_Z = \ldots$$
$$\ldots = -SIR \bullet \left|Z_L\right| \bullet \Delta i_Z \quad (24)$$

where SIR is the source-to-line impedance ratio.

Fig. 9 shows the element operating characteristic on the Δv versus $|Z_L|\Delta i_Z$ plane [11] [12].

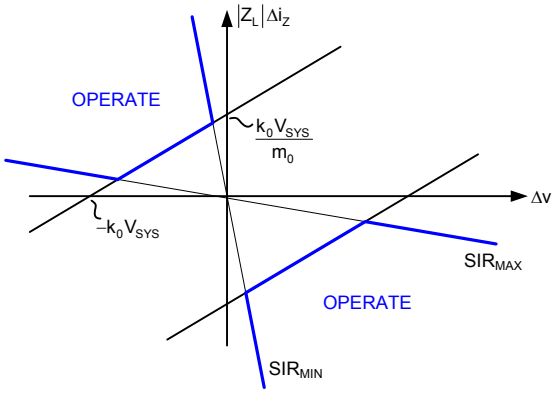

Fig. 9. Operating characteristic of the underreaching element (22) with directional supervision.

The described underreaching element is not dependable for all faults. It will not detect faults that create a small change in the fault point voltage, such as high-resistance faults. Also, the element may be slower than quarter of a cycle for faults that occur close to the voltage zero crossing. Yet, the element operates for a fair percentage of line faults and is generally very fast.

When applied on series-compensated lines, the element will be affected by series compensation but only after a power cycle or so. The element can be secured if we allow it to operate within milliseconds and inhibit it later.

CCVTs will reduce the amplitude and the steepness of the incremental voltage. However, they typically do not invert the sign of the incremental voltage or increase its amplitude. Careful analysis of (22) allows us to conclude that CCVTs may impact the dependability of this element but will not impact its security.

E. Supervisory Overreaching Element

We need an overreaching element to supervise directional elements to improve security by limiting their naturally long reach. We can modify (22) to obtain a simple supervisory overreaching element.

We want this element to reach beyond the remote line terminal up to the m_1 point ($m_1 > 1$ pu) and to respond to faults that generate a relatively small change $k_1 \bullet V_{SYS}$ in the voltage ($k_1 < 1$, such as $k_1 = 0.1$). Under this assumption, the operating equation of the overreaching supervisory element becomes:

$$\left|\Delta v - m_1 \bullet \left|Z_L\right| \bullet \Delta i_Z\right| > k_1 \bullet V_{SYS} \quad (25)$$

Fig. 10 depicts the operating characteristic of this overreaching nondirectional element on the incremental voltage versus incremental replica current plane.

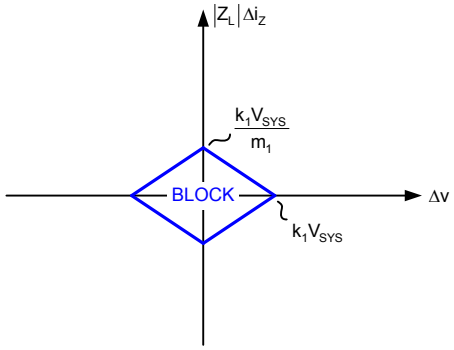

Fig. 10. Operating characteristic of the overreaching nondirectional element (25).

F. Directional Element Based on Step Changes in Voltage and Current

In the first millisecond or so of the fault, the transmission line has a purely resistive behavior (characteristic impedance), which is revealed in the relationship between the incremental voltage and the incremental current. We can understand this relationship by applying a step change in the Δv_F voltage to the network of Fig. 5 (even including line capacitance) to simulate a fault. Initially, the current follows the step change in the voltage. Later, the system starts ringing with its own natural frequencies. For a very short initial period of time, the voltage and current changes are related to the fault direction: the two signals have opposite polarities for forward faults and the same polarity for reverse faults. Hence, we can design a simple directional element that checks the relative polarities of the incremental voltage (Δv) and the incremental current (Δi). Note that this element uses the incremental current, not the incremental replica current.

Fig. 11 illustrates the operation of this directional element, originally introduced by Chamia and Liberman [8].

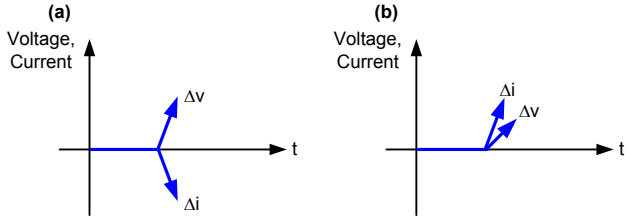

Fig. 11. Operation principle of the directional element based on step changes in voltage and current for forward (a) and reverse (b) faults.

This element must be inhibited (within 1 to 2 milliseconds after the fault) before it becomes considerably inaccurate as the system response changes from the purely resistive behavior model to the resistive-inductive behavior model and as the incremental replica current starts to describe the system better than the incremental current. In this stage, the directional element described in Subsection C is accurate.

As mentioned before, CCVTs will reduce the amplitude and the steepness of the incremental voltage, but they do not

invert its sign. As a result, CCVTs may impact the dependability of this directional element but not its security.

G. Fault Loop Considerations

The previous subsections explain several time-domain protection principles based on incremental quantities using a single-phase system representation. For practical implementation, we need to consider proper fault loop quantities for the element behavior to be independent from the fault type in actual three-phase power systems.

We are familiar with the fault loops in the frequency domain, and we will leverage the frequency domain to time-domain transformation from Subsection B to derive fault loops in the time domain.

For an AG fault, the voltage drop in the A phase across the faulted line section in the frequency domain is:

$$V_A = Z_1 I_1 + Z_1 I_2 + Z_0 I_0 \tag{26}$$

We rearrange this expression to obtain a relationship between the phase voltage V_A, the positive-sequence impedance Z_1, and a new current I_{AG} that we refer to as a "loop current":

$$V_A = Z_1 I_{AG} \tag{27}$$

The loop current that makes (26) conform with the format of (27) is therefore:

$$I_{AG} = I_A \bullet 1\angle\Theta_1 - I_0 \bullet 1\angle\Theta_1 + \frac{|Z_0|}{|Z_1|} I_0 \bullet 1\angle\Theta_0 \tag{28}$$

where Θ_0 and Θ_1 are the angles of the zero- and positive-sequence line impedances (Z_0 and Z_1), respectively.

Note that the replica current (6) is effectively a voltage drop across an RL circuit with the gain selected to be 1 at the nominal system frequency. Therefore, we can restate (6) as the following function:

$$f_{IZ}(\Delta i, R, L) = D_0(R, L) \bullet \Delta i + D_1(R, L) \bullet \frac{d}{dt}\Delta i \tag{29}$$

where D_0 and D_1 are given by (7).

Now we can rewrite (28) in the time domain as follows:

$$i_{AG} = f_{IZ}(i_A, R_1, L_1) - f_{IZ}(i_0, R_1, L_1) + \frac{|Z_0|}{|Z_1|} f_{IZ}(i_0, R_0, L_0) \tag{30}$$

where R_1, R_0, L_1, and L_0 are the resistance and inductance of the positive- and zero-sequence line impedances.

To optimize our implementation, we first calculate the following signals:

$$\Delta i_0 = \frac{1}{3}(\Delta i_A + \Delta i_B + \Delta i_C) \tag{31}$$

$$\Delta i_{0Z} = f_{IZ}(i_0, R_1, L_1) - \frac{|Z_0|}{|Z_1|} f_{IZ}(i_0, R_0, L_0) \tag{32}$$

$$i_{AZ} = f_{IZ}(i_A, R_1, L_1) \tag{33}$$

$$i_{BZ} = f_{IZ}(i_B, R_1, L_1) \tag{34}$$

$$i_{CZ} = f_{IZ}(i_C, R_1, L_1) \tag{35}$$

Then we can form the loop voltages and currents as per Table I.

TABLE I
LOOP VOLTAGES AND CURRENTS IN THE TIME DOMAIN

Loop	Voltage	Current
AG	Δv_A	$\Delta i_{AZ} - \Delta i_{0Z}$
BG	Δv_B	$\Delta i_{BZ} - \Delta i_{0Z}$
CG	Δv_C	$\Delta i_{CZ} - \Delta i_{0Z}$
AB	$\Delta v_A - \Delta v_B$	$\Delta i_{AZ} - \Delta i_{BZ}$
BC	$\Delta v_B - \Delta v_C$	$\Delta i_{BZ} - \Delta i_{CZ}$
CA	$\Delta v_C - \Delta v_A$	$\Delta i_{CZ} - \Delta i_{AZ}$

With the application of loop quantities, we make sure the elements work properly for all fault types. For example, an underreaching element based on (22) has a constant (fault type-independent) reach when using the proper voltages and currents according to Table I.

H. Phase Selection

To complete our protection algorithms, we need a phase selection algorithm. The outlined calculations are run on loop quantities, and only the output from the correct loop (for a given fault type) is allowed. As a rule, the faulted phases have the highest incremental quantities. A simple comparison between incremental quantities, such as the operating signals of (11), calculated for each of the loops allows selection of the faulted phases [6].

IV. TRAVELING WAVE-BASED LINE PROTECTION

Removing bandwidth restrictions to measure voltages and currents at the line terminals and increasing the communications data rate to exchange these measurements among line terminals allow for considerable improvements in speed. The following techniques and algorithms use fault-generated TW information [13] [14] [15].

A. Traveling Wave Principles

A fault on a transmission line generates TWs that propagate from the fault location to the line terminals with a propagation velocity that depends on the distributed inductance and capacitance of the line. Fig. 12 shows the equivalent circuit of a segment with length Δx of a two-conductor transmission line. The circuit includes resistance R, inductance L, conductance G, and capacitance C of the line in per unit of the total line length.

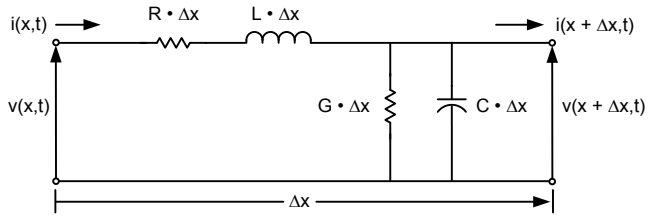

Fig. 12. Equivalent circuit of a segment of a two-conductor transmission line.

Equations (36) and (37) determine the voltage and current as a function of wave position (*x*) and time (*t*) for a two-conductor lossless transmission line in the time domain as the length of the segment Δx approaches zero. The negative sign indicates that the amplitudes of the waves decrease as *x* increases.

$$\frac{\partial v(x,t)}{\partial x} = -L\frac{\partial i(x,t)}{\partial t} \tag{36}$$

$$\frac{\partial i(x,t)}{\partial x} = -C\frac{\partial v(x,t)}{\partial t} \tag{37}$$

We differentiate (36) and (37) with respect to time and position and obtain the wave equations (38) and (39).

$$\frac{\partial^2 v(x,t)}{\partial x^2} = L\,C\frac{\partial^2 v(x,t)}{\partial t^2} \tag{38}$$

$$\frac{\partial^2 i(x,t)}{\partial x^2} = L\,C\frac{\partial^2 i(x,t)}{\partial t^2} \tag{39}$$

Equations (40) and (41) are the corresponding general solutions for the second-order partial differential equations (38) and (39) in the time domain that include forward F(x – u • t) and backward f(x + u • t) waves:

$$v(x,t) = F(x - u\bullet t) + f(x + u\bullet t) \tag{40}$$

$$i(x,t) = \frac{1}{Z_0}\bullet\left[F(x - u\bullet t) - f(x + u\bullet t)\right] \tag{41}$$

where:

$Z_0 = \sqrt{\frac{L}{C}}$ is the characteristic impedance of the line.

$u = \frac{1}{\sqrt{LC}}$ is the propagation velocity.

Wave separation techniques can be applied to extract the forward wave F(x – u • t) and the backward wave f(x + u • t).

We obtain the forward wave by multiplying (41) by Z_0 and adding it to (40). This wave depends on the line characteristic impedance Z_0 but is independent from the termination impedance.

$$v(x,t) + Z_0\bullet i(x,t) = 2\,Z_0\bullet F(x - u\bullet t) \tag{42}$$

Similarly, we can use (43) to extract the backward wave from the measured terminal quantities.

$$v(x,t) - Z_0\bullet i(x,t) = 2\,Z_0\bullet f(x + u\bullet t) \tag{43}$$

In the faulted circuit in Fig. 13, the fault current wave i_{FS} and the fault voltage wave v_{FS} travel toward Terminal S. The incident wave that is traveling from the fault to Terminal S can be calculated using (44):

$$\begin{aligned} &v_S(x,t+\tau_S) - Z_0\bullet i_S(x,t+\tau_S) = \\ &v_{FS}(x,t) + Z_0\bullet i_{FS}(x,t) \end{aligned} \tag{44}$$

where τ_S is the travel time of the wave from the fault to Terminal S and currents flowing into the line are considered to be positive.

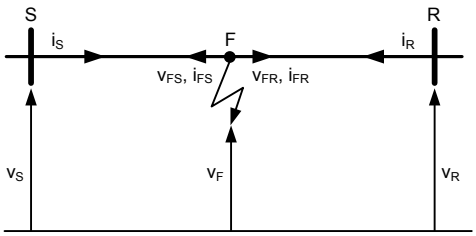

Fig. 13. Faulted line showing waves traveling from the fault toward the line terminals.

B. Traveling Wave Scheme Based on the Incident Wave Amplitudes

Let us assume that the prefault voltage at the fault point is $V_P \bullet \sin(\omega \bullet t + \theta)$, where ω is the system frequency and θ is the fault incidence angle. Then the voltage at the fault point is $v_F(t) = -V_P \bullet \sin(\omega \bullet t + \theta)$. The incident wave at Terminal S is calculated using (44) and given in (45).

$$v_S(t+\tau_S) - Z_0\bullet i_S(t+\tau_S) = -2\bullet V_P\bullet\sin(\omega\bullet t+\theta) \tag{45}$$

The wave given in (45) is termination-independent, but it depends on the fault incidence angle. To make it independent of the fault incidence angle, Dommel introduced a discrimination factor D based on (46) through (49) [16].

Taking the time derivative of (45), we get:

$$\begin{aligned} &\frac{1}{\omega}\frac{d}{dt}\left[v_S(t+\tau_S) - Z_0\bullet i_S(t+\tau_S)\right] = \\ &-2\bullet V_P\bullet\cos(\omega\bullet t+\theta) \end{aligned} \tag{46}$$

Squaring (45) and (46), we obtain:

$$\begin{aligned} &\left[v_S(t+\tau_S) - Z_0\bullet i_S(t+\tau_S)\right]^2 = \\ &4\bullet V_P{}^2\bullet\sin^2(\omega\bullet t+\theta) \end{aligned} \tag{47}$$

$$\begin{aligned} &\left\{\frac{1}{\omega}\frac{d}{dt}\left[v_S(t+\tau_S) - Z_0\bullet i_S(t+\tau_S)\right]\right\}^2 = \\ &4\bullet V_P{}^2\bullet\cos^2(\omega\bullet t+\theta) \end{aligned} \tag{48}$$

Adding (47) and (48), we get a value (discriminant D) independent from the fault incident angle:

$$D = 4 \bullet V_P{}^2 = \left[v_S(t+\tau_S) - Z_0 \bullet i_S(t+\tau_S) \right]^2 + \frac{1}{\omega^2}\left[\frac{dv_S(t+\tau_S)}{dt} - Z_0 \bullet \frac{di_S(t+\tau_S)}{dt} \right]^2 \quad (49)$$

Because the D factor comprises incident waves, the D values are large for forward faults and near zero for reverse faults. A communications-based comparison scheme is used to make sure the D values are large at both line terminals, and if so, the line is tripped. The described method works with a traditional low-bandwidth communications channel, but it needs high-fidelity voltage signals, which generally cannot be provided by CCVTs.

C. Directional Comparison Scheme Based on Incident and Reflected Traveling Waves

We can compare the incident and reflected TWs to make directional tripping decisions. The algorithm described in this subsection calculates the incident (forward) and reflected (backward) TWs using (50) and (51), respectively.

$$s_F = v(t) - Z_0 i(t) \quad (50)$$

$$s_B = v(t) + Z_0 i(t) \quad (51)$$

The sequence in which the incident and reflected waves exceed a predefined threshold determines the fault direction. For forward faults, the incident wave appears before the reflected wave, assuming that it takes some time for the wave to reach a discontinuity behind the relay and travel back toward the line terminal. For a reverse fault, the reverse direction wave from the fault appears long before the wave reflected from the remote terminal returns to the relay location as a forward wave. A directional comparison scheme using this TW directional element is applied to trip the line.

The method was originally proposed by Johns in [17] and is a straightforward application of the wave separation theory. The wave separation method uses a traditional low-bandwidth communications channel, but it requires high-fidelity voltage measurements.

D. Distance to Fault Element Based on Traveling Waves

With reference to Fig. 14, the TW launched by the fault is reflected at the relay location. The reflected TW travels to the fault, is reflected at the fault point, and returns to the relay location. We can design an underreaching TW distance element by measuring the time difference Δt between the arrival of the first TW from the fault and the arrival of the TW reflected at the fault point. The element calculates the fault distance using Δt and the wave propagation velocity and issues a trip if the distance is shorter than the set reach.

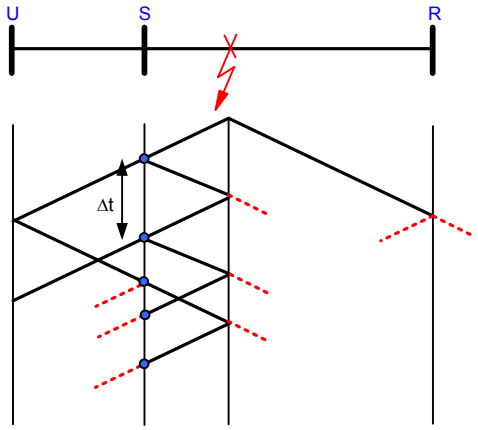

Fig. 14. Using multiple reflections to calculate the distance to the fault.

The following steps summarize the distance-to-fault calculation:

- Upon arrival of the first TW to the line terminal, determine the fault direction using a directional element similar to the one proposed by [17].
- For faults in the forward direction, estimate Δt between the two TWs, as shown in Fig. 14. The method can use cross-correlation to verify similarity of the wave reflected from the fault and the prior wave traveling toward the fault.
- Calculate the distance to the fault using $d = \frac{\Delta t}{2} \bullet u$.
- Trip if d is less than a reach setting.

The distance measurement method was originally proposed by Crossley [18]. Note that the first few waves can create similar patterns at various line terminals. For example, the first waves recorded at Terminal S and Terminal U are very similar in terms of polarity and relative timing. While Terminal S is expected to trip, Terminal U is expected to block. Reference [18] claims selective operation based on checking the similarity between the TW shapes.

E. Traveling Wave Differential Scheme

When we neglect the effects of dispersion and attenuation, the incident waves at the local terminal delayed by the line propagation time (τ) equal the incident waves at the remote terminal, if there is no fault on the protected line.

This observation can be turned into a relay algorithm by using Bergeron's equations (52) and (53) [19].

$$i_S(t-\tau) + \frac{1}{Z_0} \bullet v_S(t-\tau) = -i_R(t) + \frac{1}{Z_0} \bullet v_R(t) \quad (52)$$

$$-i_S(t) + \frac{1}{Z_0} \bullet v_S(t) = i_R(t-\tau) + \frac{1}{Z_0} \bullet v_R(t-\tau) \quad (53)$$

Equations (52) and (53) are balanced for external faults and switching events, and they become unbalanced for internal faults. Therefore, we can define differential signals based on (52) and (53) and use the non-zero values of the differential signals for tripping:

$$\varepsilon_S = i_S(t-\tau) + i_R(t) + \frac{1}{Z_0}\left[v_S(t-\tau) - v_R(t)\right] \quad (54)$$

$$\varepsilon_R = i_R(t-\tau) + i_S(t) + \frac{1}{Z_0}\left[v_R(t-\tau) - v_S(t)\right] \quad (55)$$

This method was originally introduced by Takagi in [19] and [20] and constitutes a differential element based on incident TWs. It requires high-bandwidth communications and precise time alignment between the line terminals. Last, but not least, it requires high-fidelity voltage signals to calculate the incident waves before comparing their values.

F. Current-Only Traveling Wave Differential Scheme

We can eliminate the requirement for high-fidelity voltage signals discussed in the previous subsection by implementing a current-only TW differential scheme that compares the amplitudes of the measured current waves.

For external faults, the amplitudes of the measured current waves would not match perfectly between the line terminals not only because of line attenuation but also because of the line termination effects. Isolating incident and reflected waves makes the measurement independent of the termination impedances, as in the Takagi method, allowing comparison of the TWs between the line terminals, but it requires high-fidelity voltage information.

However, the measured current waves, which are the sums of the incident and reflected waves, retain the polarity information of the incident waves. Therefore, we can compare the measured current waves at both line terminals, taking into account the line propagation delay.

The principle follows these steps:

- We assume an internal fault and add the first current TWs that arrived at the local and remote terminals (properly time aligned) to calculate an operating quantity. If this quantity is significant (indicating an internal fault), we proceed to the second step to confirm that the fault is not external.
- We assume an external fault and calculate the through-current TW, recognizing that for external faults, the current TW that entered at one line terminal will leave at the other terminal after the line propagation time delay, τ, and the restraining quantity will have a large value.
- We compare the operating and restraining quantities to make a tripping decision.

We formalize the first step using the following operating quantity:

$$i_{OP(t)} = \left| i_{S(t)} + i_{R(t-P)} \right| \quad (56)$$

where $P \leq \tau$ is the time shift we need to align the first current TW received at Terminal R with the first current TW received at Terminal S.

Equation (56) assumes the Terminal R TW arrived first. If the Terminal S TW arrived first, we need to delay the Terminal S TW:

$$i_{OP(t)} = \left| i_{S(t-P)} + i_{R(t)} \right| \quad (57)$$

Either (56) or (57) is executed, depending on which terminal received the TW first. These equations are executed only once, giving a single value (i_{OP}) that approximately equals the current TW launched from the fault location. For internal faults, the two TWs have the same polarities, yielding a large i_{OP} value.

We formalize the second step using the following equations for the restraining quantities:

$$i_{RT1(t)} = \left| i_{S(t)} - i_{R(t-\tau)} \right| \quad (58)$$

$$i_{RT2(t)} = \left| i_{R(t)} - i_{S(t-\tau)} \right| \quad (59)$$

Equation (58) is executed once at the point in time τ after the first TW arrives at Terminal R.

Similarly, (59) is executed once at the point in time τ after the first TW arrives at Terminal S.

For external faults, the Terminal S and Terminal R TW currents have opposite polarities, yielding large i_{RT1} and i_{RT2} values.

We combine the two restraining quantities, for example, using:

$$i_{RT} = \max\left(i_{RT1}, i_{RT2}\right) \quad (60)$$

or

$$i_{RT} = \frac{1}{2}\left(i_{RT1} + i_{RT2}\right) \quad (61)$$

The element operates if:

$$i_{OP} > k \bullet i_{RT} \quad (62)$$

where *k* is a restraining factor.

This current-only scheme requires high-speed communications and the capability to align the data from both terminals.

For illustration, consider internal and external BG faults on a 189-mile transmission line with a propagation time delay of 1.03 milliseconds. In the following figures, we plotted the Terminal S (red) and Terminal R (blue) B-phase alpha current

TWs obtained using a differentiator-smoother filter (see [13]) having a window length of 20 microseconds.

Fig. 15 shows an external fault close to Terminal S. The current TW entered the protected line at Terminal S at 30.20 milliseconds with a value of around +462 A and left the line at Terminal R at 31.23 milliseconds with a value of around –464 A. The operating signal calculated using (57) with the time shift of P = 1.03 milliseconds equals around 2 A. The restraining signal calculated using (59) and (60) equals around 926 A. The restraining signal (926 A) is much greater than the operating signal (2 A), and the element restrains as expected.

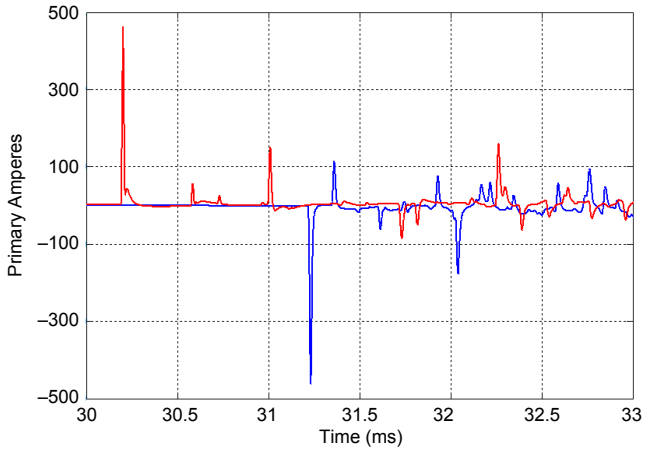

Fig. 15. Current TWs at Terminal S (red) and Terminal R (blue) for an external fault close to Terminal S.

Fig. 16 shows an external fault in the power system located at a similar distance with respect to Terminal S and Terminal R (for example, a fault on a parallel line with a separate right of way). As a result, the first TWs arrived at Terminal S and Terminal R with the same polarity and only around 0.2 milliseconds apart. The operating signal calculated for P = 0.2 milliseconds equals around 403 A + 219 A = 622 A. This case could be mistaken for an internal fault. Notice that the Terminal S TW that entered at around 30.50 milliseconds with an amplitude of 403 A left Terminal R at around 31.53 milliseconds with an amplitude of –411 A. Similarly, the TW that entered Terminal R at around 30.65 milliseconds with an amplitude of 219 A left Terminal S at 31.68 milliseconds with an amplitude of –208 A. Therefore, the restraining signals are 403 – (–411) = 814 A and 219 – (–208) = 427 A. The total restraining signal per (60) is 814 A. Because the restraining signal (814 A) is greater than the operating signal (622 A), the element restrains as expected (using k = 1).

Fig. 17 shows an internal fault at 69.2 miles from Terminal R. The operating signal for this case is around 960 + 785 = 1,745 A. The restraining signals are around 960 A and 785 A, respectively, because the initial waves do not leave the line after the line propagation time. The total restraining signal is therefore around 960 A. As a result, the operating signal (1,745 A) is much greater than the restraining signal (960 A), and the element operates dependably.

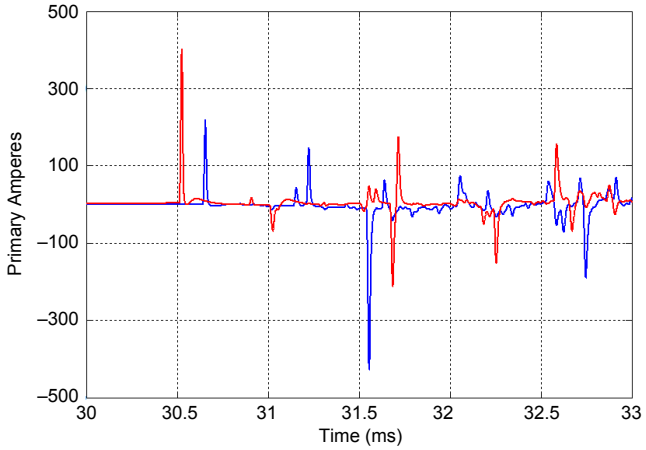

Fig. 16. Current TWs at Terminal S (red) and Terminal R (blue) for an external fault at a similar distance from Terminal S and Terminal R.

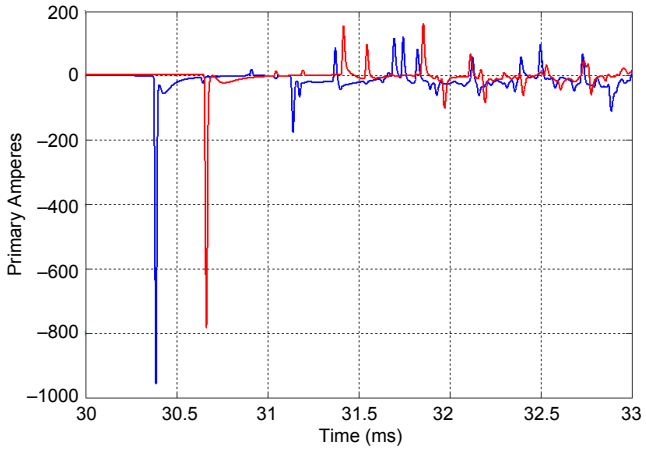

Fig. 17. Current TWs at Terminal S (red) and Terminal R (blue) for an internal fault at 69.2 miles from Terminal R.

V. Can Protection Be Too Fast?

Ultra-high-speed line protection has a chance to see events on the protected transmission line other than short circuits caused by catastrophic insulation breakdowns. Examples of such events include:

- Normal operation of in-line surge arresters due to overvoltages caused by switching events or external faults.
- Opening or closing the bypass breaker on in-line series capacitors (insertion or removal of series compensation).
- Lightning strikes to ground wires and towers that induce TWs on power conductors that travel toward the line terminals.
- Parallel line faults that induce TWs in the protected line that travel toward the line terminals.

Today's protection schemes are too slow or not sensitive enough to respond to these events. As a result, we may not be fully aware of the rate of occurrence and variety of these events.

The ultra-high-speed line protection, like any protection, must be designed not to respond to these events if they are external events. However, if the event is located on the

protected line, the distinction between a short circuit that requires tripping and normal arrester conduction, for example, is challenging.

Two groups of solutions to this security challenge can be applied.

First, a legitimate short circuit dissipates a certain amount of energy during the air insulation breakdown. We can measure the amount of energy traveling toward the event location using incremental voltages and currents. In addition, we can measure the current derivative to determine not only the current amplitude but also how quickly it increases. As a result, we can estimate the severity of the event using 1 to 2 milliseconds of data for proper trip supervision.

Second, specific supervisory conditions can be developed to cope with specific events. Let us consider normal arrester conduction due to an overvoltage condition. Fortunately, surge arresters are normally installed at the line terminals, and therefore, at least one relay has access to the arrester voltage. We can monitor the voltage on a sample-by-sample basis to see if it exceeds the conduction threshold of a normally operating arrester. If it does, we attribute the resulting current to the normal conduction of the arrester and do not trip the line. However, if the current does not subside, we need to suspect an arrester failure and trip the protected line.

We expect a short learning period for the ultra-high-speed line protection technology as we characterize these events and incorporate dedicated supervisory conditions for security.

VI. Conclusions

Most protection elements today use voltage and current phasors, i.e., they operate on steady-state fault signal components. These elements need a data window of about one cycle to measure the phasors accurately enough for secure protection. Some protection elements, such as switch-onto-fault or directional elements, can tolerate larger transient errors and therefore can use shorter data windows.

To break free of phasor limitations, we need to base protection element operation on instantaneous voltages and currents. These signal components require shorter data windows, facilitating faster protection.

One way to develop faster line protection is to use the differential equations that describe a lumped parameter RL circuit representing the protected line and the surrounding system. This RL representation is accurate below a few hundred hertz. Using this frequency spectrum in the instantaneous voltages and currents, we can speed up protection to about a quarter of a cycle for a wide range of favorable system and fault conditions. These methods work with traditional CCVTs.

Protection methods based on TWs are another time-domain approach. These methods are based on the distributed parameter line and system model and take advantage of the frequency spectrum above a hundred kilohertz with a potential for 1-millisecond operating times. Some of these methods require high-fidelity voltages and currents. CTs allow measuring current TWs, but CCVTs are not adequate for voltage TW measurements. The need for high-fidelity voltage information calls for high-bandwidth voltage sensors and creates an obstacle in the application of TW-based protection methods that use high-fidelity voltage information.

A novel TW current-only differential element presented in this paper eliminates the high-fidelity voltage requirement. It uses high-speed communications, which are easier to achieve today with the widespread availability of fiber-optic channels as compared with installing new high-voltage measuring devices.

Combining the lumped parameter circuit-based and TW-based time-domain approaches allows for versatile applications covering various relay input voltage sources and available communications channels.

After years of steady development, modern electronic components have reached the processing power levels necessary to implement even the most demanding protection algorithms. This includes the ability to economically support high sampling rates (≥1 MHz), high-resolution (≥16 bits) synchronized sampling, absolute time synchronization, communications capable of exchanging all acquired data (≥100 Mbps), or high numeric burden required by some of the algorithms (≥1 G multiplications per second).

Today, we face no major limitations preventing us from improving line relaying speed and breaking free of phasor limitations.

VII. References

[1] R. B. Eastvedt, "The Need for Ultra-Fast Fault Clearing," proceedings of the Third Annual Western Protective Relay Conference, Spokane, WA, October 1976.

[2] E. O. Schweitzer, III, and D. Hou, "Filtering for Protective Relays," proceedings of the 19th Annual Western Protective Relay Conference, Spokane, WA, October 1992.

[3] E. O. Schweitzer, III, "New Developments in Distance Relay Polarization and Fault Type Selection," proceedings of the 16th Annual Western Protective Relay Conference, Spokane, WA, October 1989.

[4] E. O. Schweitzer, III, "Computationally-Efficient Distance Relay for Power Transmission Lines," U.S. Patent 5,325,061, June 1994.

[5] E. O. Schweitzer, III, and J. Roberts, "Distance Relay Element Design," proceedings of the 19th Annual Western Protective Relay Conference, Spokane, WA, October 1992.

[6] A. Guzmán, J. Mooney, G. Benmouyal, and N. Fischer, "Transmission Line Protection System for Increasing Power System Requirements," proceedings of the 55th Annual Conference for Protective Relay Engineers, College Station, TX, April 2002.

[7] M. G. Adamiak, G. E. Alexander, and W. Premerlani, "A New Approach to Current Differential Protection for Transmission Lines," proceedings of the 53rd Annual Georgia Tech Protective Relaying Conference, Atlanta, GA, May 1999.

[8] M. Chamia and S. Liberman, "Ultra High Speed Relay for EHV/UHV Transmission Lines – Development, Design, and Application," *IEEE Transactions on Power Apparatus and Systems*, Vol. PAS–97, Issue 6, November 1978, pp. 2104–2116.

[9] M. T. Yee and J. Esztergalyos, "Ultra High Speed Relay for EHV/UHV Transmission Lines – Installation-Staged Fault Tests and Operational Experience," *IEEE Transactions on Power Apparatus and Systems*, Vol. PAS–97, No. 5, September/October 1978, pp. 1814–1825.

[10] K. Zimmerman and D. Costello, "Fundamentals and Improvements for Directional Relays," proceedings of the 63rd Annual Conference for Protective Relay Engineers, College Station, TX, March/April 2010.

[11] F. Engler, O. E. Lanz, M. Hanggli, and G. Bacchini, "Transient Signals and Their Processing in an Ultra High-Speed Directional Relay for EHV/UHV Transmission Line Protection," *IEEE Transactions on Power Apparatus and Systems*, Vol. PAS–104, No. 6, June 1985, pp.1463–1473.

[12] M. Vitins, "A Fundamental Concept for High Speed Relaying," *IEEE Transactions on Power Apparatus and Systems*, Vol. PAS–100, Issue 1, January 1981, pp. 163–173.

[13] E. O. Schweitzer, III, A. Guzmán, M. V. Mynam, V. Skendzic, B. Kasztenny, and S. Marx, "Locating Faults by the Traveling Waves They Launch," proceedings of the 40th Annual Western Protective Relay Conference, Spokane, WA, October 2013.

[14] M. Ando, E. O. Schweitzer, III, and R. A. Baker, "Development and Field-Data Evaluation of Single-End Fault Locator for Two-Terminal HVDC Transmission Lines, Part I: Data Collection System and Field Data," *IEEE Transactions on Power Apparatus and Systems*, Vol. PAS–104, Issue 12, December 1985, pp. 3524–3530.

[15] M. Ando, E. O. Schweitzer, III, and R. A. Baker, "Development and Field-Data Evaluation of Single-End Fault Locator for Two-Terminal HVDC Transmission Lines, Part II: Algorithm and Evaluation," *IEEE Transactions on Power Apparatus and Systems*, Vol. PAS–104, Issue 12, December 1985, pp. 3531–3537.

[16] H. W. Dommel and J. M. Michels, "High Speed Relaying Using Traveling Wave Transient Analysis," *IEEE Power Engineering Society Winter Meeting*, New York, Paper No. A78, January/February 1978, pp. 214–219.

[17] A. T. Johns, "New Ultra-High-Speed Directional Comparison Technique for the Protection of EHV Transmission Lines," *IEE Proceedings C: Generation, Transmission, and Distribution*, Vol. 127, Issue 4, July 1980, pp. 228–239.

[18] P. A. Crossley and P. G. McLaren, "Distance Protection Based on Travelling Waves," *IEEE Transactions on Power Apparatus and Systems*, Vol. PAS–102, Issue 9, September 1983.

[19] T. Takagi, J. Barbar, U. Katsuhiko, and T. Sakaguchi, "Fault Protection Based on Travelling Wave Theory, Part I: Theory," *IEEE Power Engineering Society Summer Meeting*, Mexico, Paper A77, July 1977, pp. 750–753.

[20] T. Takagi, Y. Yamakosi, M. Yamaura, R. Kondow, T. Matsushima, and M. Masui, "Digital Differential Relaying System for Transmission Line Primary Protection Using Traveling Wave Theory – Its Theory and Field Experience," *IEEE Power Engineering Society Winter Meeting*, New York, Paper A79, January/February 1979, pp. 1–9.

VIII. BIOGRAPHIES

Dr. Edmund O. Schweitzer, III, is recognized as a pioneer in digital protection and holds the grade of Fellow in the IEEE, a title bestowed on less than one percent of IEEE members. In 2002, he was elected as a member of the National Academy of Engineering. Dr. Schweitzer received the 2012 Medal in Power Engineering, the highest award given by IEEE, for his leadership in revolutionizing the performance of electrical power systems with computer-based protection and control equipment. Dr. Schweitzer is the recipient of the Graduate Alumni Achievement Award from Washington State University and the Purdue University Outstanding Electrical and Computer Engineer Award. He has also been awarded honorary doctorates from both the Universidad Autónoma de Nuevo León, in Monterrey, Mexico, and the Universidad Autónoma de San Luis Potosí, in San Luis Potosí, Mexico, for his contributions to the development of electric power systems worldwide. He has written dozens of technical papers in the areas of digital relay design and reliability, and holds 100 patents worldwide pertaining to electric power system protection, metering, monitoring, and control. Dr. Schweitzer received his bachelor's and master's degrees in electrical engineering from Purdue University, and his doctorate from Washington State University. He served on the electrical engineering faculties of Ohio University and Washington State University, and in 1982, he founded Schweitzer Engineering Laboratories, Inc. (SEL), to develop and manufacture digital protective relays and related products and services. Today, SEL is an employee-owned company that serves the electric power industry worldwide and is certified to the international quality standard ISO9001:2008. SEL equipment is in service at voltages from 5 kV through 500 kV to protect feeders, motors, transformers, capacitor banks, transmission lines, and other power apparatus.

Bogdan Kasztenny is the R&D director of technology at Schweitzer Engineering Laboratories, Inc. He has over 25 years of experience in power system protection and control, including 10 years of academic career and 15 years of industrial experience, developing, promoting, and supporting many protection and control products. Dr. Kasztenny is an IEEE Fellow, Senior Fulbright Fellow, Canadian representative of CIGRE Study Committee B5, registered professional engineer in the province of Ontario, and an adjunct professor at the University of Western Ontario. Since 2011, Dr. Kasztenny has served on the Western Protective Relay Conference Program Committee. Dr. Kasztenny has authored about 200 technical papers and holds 25 patents.

Armando Guzmán received his BSEE with honors from Guadalajara Autonomous University (UAG), Mexico. He received a diploma in fiber-optics engineering from Monterrey Institute of Technology and Advanced Studies (ITESM), Mexico, and his MSEE and MECE from the University of Idaho, USA. He served as regional supervisor of the Protection Department in the Western Transmission Region of the Federal Electricity Commission (the electrical utility company of Mexico) in Guadalajara, Mexico, for 13 years. He lectured at UAG and the University of Idaho on power system protection and power system stability. Since 1993, he has been with Schweitzer Engineering Laboratories, Inc. in Pullman, Washington, where he is a fellow research engineer. He holds numerous patents in power system protection and metering. He is a senior member of IEEE.

Veselin Skendzic is a principal research engineer at Schweitzer Engineering Laboratories, Inc. He earned his BS in electrical engineering from FESB, University of Split, Croatia; his Masters of Science from ETF, Zagreb, Croatia; and his Ph.D. from Texas A&M University, College Station, Texas. He has more than 25 years of experience in electronic circuit design and power system protection-related problems. He is a senior member of IEEE, has written multiple technical papers, and is actively contributing to IEEE and IEC standard development. He is a member of the IEEE Power Engineering Society (PES) and the IEEE Power System Relaying Committee (PSRC) and a past chair of the PSRC Relay Communications Subcommittee (H).

Mangapathirao (Venkat) Mynam received his MSEE from the University of Idaho in 2003 and his BE in electrical and electronics engineering from Andhra University College of Engineering, India, in 2000. He joined Schweitzer Engineering Laboratories, Inc. (SEL) in 2003 as an associate protection engineer in the engineering services division. He is presently working as a senior research engineer in SEL research and development. He was selected to participate in the U.S. National Academy of Engineering (NAE) 15th Annual U.S. Frontiers of Engineering Symposium. He is a senior member of IEEE.

Previously presented at the 2015 Texas A&M Conference for Protective Relay Engineers.

20150210 • TP6673-01